Article:
Khodaparast, S, Sharratt, WN, Tyagi, G et al. (3 more authors) (2021) Pure and mixed aqueous micellar solutions of Sodium Dodecyl sulfate (SDS) and Dimethyldodecyl Amine Oxide (DDAO): Role of temperature and composition. Journal of Colloid and Interface Science, 582 (Part B). pp. 1116-1127. ISSN 1095-7103

https://doi.org/10.1016/j.jcis.2020.08.002

Pure and mixed aqueous micellar solutions of Sodium Dodecyl sulfate (SDS) and Dimethyldodecyl Amine Oxide (DDAO): role of temperature and composition

Sepideh Khodaparast[a,b,*], William N. Sharratt[a], Gunjan Tyagi[a], Robert M. Dalgliesh[c], Eric S. J. Robles[d], João T. Cabral[a,*]

[a] *Chemical Engineering Department, Imperial College London, SW7 2AZ London, United Kingdom*
[b] *School of Mechanical Engineering, University of Leeds, LS2 9JT Leeds, United Kingdom*
[c] *ISIS Neutron and Muon Source, Science and Technology Facilities Council, Rutherford Appleton Laboratory, OX11 0QX Didcot, United Kingdom*
[d] *The Procter & Gamble Company, Newcastle Innovation Centre, NE12 9TS Newcastle-Upon-Tyne, United Kingdom*

Abstract

Aqueous mixtures of anionic and nonionic/cationic surfactants can form non-trivial self-assemblies in solution and exhibit macroscopic response. Here, we investigate the micellar phase of pure and mixed aqueous solutions of Sodium Dodecyl Sulfate (SDS) and Dimethyldodecyl Amine Oxide (DDAO) using a combination of Small Angle Neutron Scattering (SANS), Fourier-Transform Infrared Spectroscopy (FTIR) and rheological measurements. We examine the effect of temperature (0-60°C), on the 20 wt% SDS micellar solutions with varying DDAO additive ($\leq$ 5 wt%), and seek to correlate micellar structure with zero-shear solution viscosity. SANS establishes the formation of prolate ellipsoidal micelles in aqueous solutions of pure SDS, DDAO and SDS/DDAO mixtures, whose axial ratio is found to increase upon cooling. Elongation of the ellipsoidal micelles of pure SDS is also induced by the introduction of the non-anionic DDAO, which effectively reduces the repulsive interactions between the anionic SDS head-groups. In FTIR measurements, the formation of elongated mixed ellipsoidal micelles is confirmed by the increase of ordering in the hydrocarbon chain tails and interaction between surfactant head-groups. We find that the zero-shear viscosity of the mixed surfactant solutions increases exponentially with decreasing temperature and increasing DDAO content. Significantly, a master curve for solution viscosity can be obtained in terms of micellar aspect ratio, subsuming the effects of both temperature and DDAO composition in the experimental range investigated. The intrinsic viscosity of mixed micellar so-

*Corresponding author
Email addresses: s.khodaparast@leeds.ac.uk (Sepideh Khodaparast), j.cabral@imperial.ac.uk (João T. Cabral)

lutions is significantly higher than the analytical and numerical predictions for Brownian suspensions of ellipsoidal colloids, highlighting the need to consider interactions of soft micelles under shear, especially at high concentrations.

Keywords: temperature, phase behaviour, mixed surfactant, Dimethyldodecyl Amine Oxide DDAO, Sodium Dodecyl sulfate SDS, viscosity, ATR-FTIR, anionic surfactant, ellipsoidal micelles, SANS.

1. Introduction

Surfactants are key components in numerous formulated mixtures with applications in food, enhanced oil recovery, agriculture and soil treatment, as well as household, cosmetic and pharmaceutical products.[1, 2, 3, 4, 5, 6, 7] For a given application, surfactants molecules and their self-assembled structures may play one or several diverse roles as detergents, foaming and wetting agents, and dispersants.[8] Almost without exception, formulated mixtures contain several types of surfactant molecules to achieve the desired stability and functionality in the final product.[9] From an academic point of view, over the past decades, mixtures of surfactants have provided both theoretical and experimental challenges in defining the links between interactions at the molecular scale and the macroscopic bulk properties of the corresponding solutions.[10, 11, 12, 13, 14]

Mixtures of anionic and nonionic/cationic surfactants are of particular scientific interest due to the (potential) synergistic interactions between dissimilarly charged head-groups, [15, 16, 17, 18] that can be exploited in practical applications. Typically, upon mixing surfactants of differing head-group charge, (i) the Critical Micelle Concentration (CMC) of the solution is significantly reduced compared to predictions for ideal micelles, (ii) relatively larger micelles with modified shapes are formed, (iii) the temperature-concentration equilibrium phase boundaries between the micellar and liquid crystalline and/or crystalline phases are shifted and (iv) viscosity of the mixed solution significantly increases compared to that of individual surfactant solutions at similar total surfactant concentrations.[19, 20, 21, 22, 23, 18, 24, 25, 26]

Here, we investigate the effect of adding an amphoteric surfactant Dimethyldodecyl Amine Oxide (DDAO) to a commonly used anionic surfactant Sodium Dodecyl sulfate (SDS), a combination that is often found in liquid detergents.[27, 26] Amphoteric surfactants are a class of surface active agents that carry a net charge which is sensitive to both pH of the solution and the presence of other surfactants in the mixture. In particular, for DDAO molecules, the amine oxide group exists in either a nonionic (at pH$>$ 7) or cationic (at pH$<$ 5) form due to protonation of the oxygen atom in the amine oxide head-group.[28] When added to anionic surfactants, DDAO has been found to promote the formation of mixed micelles, significantly reduce the CMC and modify the shape, charge and aggregation number of the micelles.[29, 30, 31, 32] In this work, we focus on the micelles formed in mixtures of DDAO and SDS in pure water, without altering the PH of the solution through addition of acid or base. The pH of

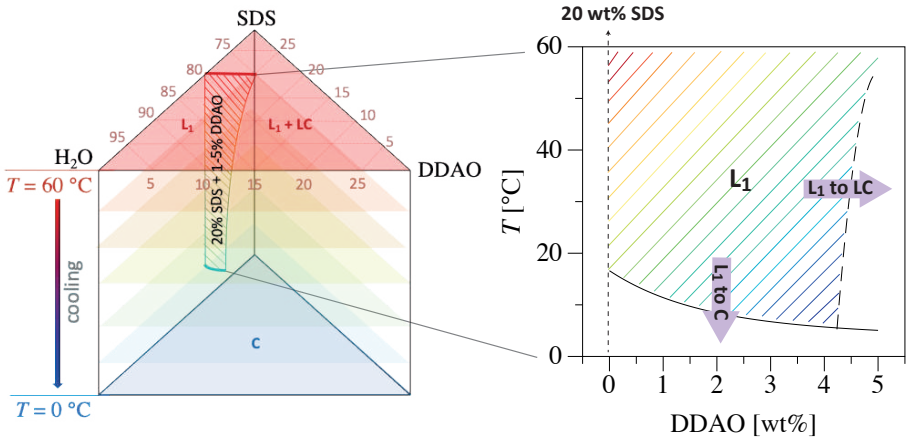

Figure 1: Investigated range of compositions and temperature within the ternary phase map of SDS/DDAO/water.[22] Aqueous binary solutions of SDS and DDAO, with concentrations below 30 wt%, as well as mixtures with fixed concentration of SDS (20 wt%) and varying concentrations of DDAO (1-5 wt%), were studied within 0-60 °C. Mixed SDS/DDAO/water solutions reside in the micellar phase (L_1) at 60 °C. Upon cooling the mixtures down to room temperature, solutions with higher DDAO content ($\geq$ 5 wt%) form a liquid crystalline phase (LC), whilst others with lower DDAO content remain in the L_1 phase. At lower temperatures ($T = 0$ °C), a single crystalline phase (C) or coexisting L_1, LC and C phases may exist, which are highly dependent on the DDAO content.

the solutions remains around 7 and above, for which DDAO alone would be expected to behave as a nonionic surfactant.

Previously, structural analyses of mixed DDAO and SDS micellar systems have predominately focused on lower total surfactant concentrations ($<$ 10 wt%).[31] In general, relatively elongated micelles, compared to pure micelles of either SDS or DDAO, were found to form in mixed DDAO/SDS systems. Incorporation of DDAO into SDS micelles was found to decrease the net charge of the micelles, reducing the area designated for each surfactant head-group, and consequently increasing the packing parameter.[33] By contrast, the effect of added DDAO to concentrated SDS solutions, particularly in terms of the size and shape of self-assembled structures, has received considerably less attention. Based on rheological solution behaviour, Weers *et al.* (1990) reported a ternary phase diagram of C_{14}AO and SDS in water, at less than 30 wt% total surfactant concentration. Adding C_{14}AO to aqueous solutions with a fixed amount of SDS was found to promote the transition from roughly spherical micelles to elongated rods and eventually to a hexagonal liquid crystalline phase.[22] Summerton *et al.* performed Small Angle X-ray Scattering (SAXS) measurements of a SDS/DDAO mixture at a fixed concentration (20 wt% SDS and 3 wt% DDAO) and compared their findings with those obtained for pure SDS micelles (20 wt%). They found both pure and mixed systems to form prolate ellipsoidal micelles, with larger axial ratios prevalent in the latter case.[31, 34] Whilst most

studies on the micellar phase of mixed surfactants have investigated the effects of chemical additives and molar ratios of the components (mainly the surfactant mixture), the effect of temperature, and especially cooling below room temperature, is yet to be investigated in detail, despite its practical importance (e.g. in low temperature detergency).

The main goal of this study is to investigate the effect of temperature variation over a wide range of 0 °C $< T <$ 60 °C on the molecular structure and rheological response of the micellar phase of SDS, DDAO and their mixtures. We first report SANS measurements of micellar phases of pure solutions of SDS and DDAO for concentrations below 30 wt%, as they are both frequently used in applications where temperature variations may occur.[35, 36, 37, 38] We then examine mixed solutions of primarily 20 wt% SDS with varying DDAO content (1-5 wt%), see Fig. 1 for an illustration. This range of surfactant concentration and composition is chosen to: (1) thermally extend one of the most interesting areas of the ternary phase diagram of SDS/DDAO/H_2O, where minimal thermal, compositional and/or concentration fluctuations lead to dramatic mesoscopic and macroscopic changes of solution properties (Fig. 1).[22] (2) Provide a molecular underpinning to the thermal stability of model formulated detergent mixtures and their response to thermal fluctuations, particularly cooling below ambient temperature, where these mixtures often do not perform or appear as desired.

We first use Dynamic Light Scattering (DLS) and Cross-polarised Optical Microscopy (OM) to identify the temperature-concentration boundaries of the micellar phase. SANS is then employed to determine the shape, size, and net charge of micelles in pure and mixed aqueous solutions of SDS and DDAO. We combine these data with FTIR spectroscopy measurements to elucidate the synergistic interactions between the two surfactants in mixed micelles. Finally, we perform rheological measurements for pure and mixed solutions of SDS and DDAO across the desired range of temperature to highlight the effects of micellar structural changes on the viscosity of the surfactant solutions.

2. Materials and Methods

Sodium dodecyl sulfate SDS (>99.0% purity) and an aqueous solution of 30 wt% $C_{12}AO$ were purchased from Sigma-Aldrich and used as received. Solutions for DLS, OM and FTIR measurements were prepared by diluting the surfactants in deionised water. For SANS measurements, DDAO and SDS (both of >99.0% purity) were used and all solutions were prepared in D_2O. Considering the density difference between H_2O and D_2O, a correction was made when preparing samples in D_2O to keep the molar fraction of surfactant constant.

Cross-polarised Optical Microscopy (OM). Cross-polarised optical microscopy was used to detect phase transition from the isotropic micellar phase to the birefringent liquid crystalline and the crystalline phases, following procedures described in a previous publication.[39] Approximately 3 μl of the solution was placed between two thin glass cover slips. Solvent evaporation during the experiments was minimised by sealing the area surrounding the droplet using

a gasket. Isothermal experiments were performed by initially stabilizing the droplet at 60 °C before a rapid quench (at 80 °C/min) to the final temperature of interest. OM images were captured with an Olympus BX41M-LED microscope, using a 10X objective and a CMOS camera (Basler ac2040-90) that provided an overall spatial resolution of 1.5 μm per pixel.

Dynamic Light Scattering (DLS). Dynamic light scattering (DLS) was performed using a Zetasizer Nano S (Malvern Panalytical), which operates with a back-scattering detector ($\theta = 173°$) and a 633 nm He-Ne laser yielding a fixed value of $q \simeq 0.0026$ Å^{-1}. The cuvette temperature was controlled with a Peltier system in the range of 60 °C down to to 0 °C. All cooling cycles were started from 60 °C to ensure that sample were initially in the isotropic micellar phase. Data were acquired in triplicate. Time-resolved measurements, over 30 mins, were performed to probe the transition from micellar to liquid crystalline and crystalline phases. The raw correlograms could be interpreted without cumulant fitting or CONTIN analysis, in order to identify the boundaries of the micellar phase.

Small Angle Neutron Scattering (SANS). SANS experiments in linear and isothermal cooling cycles were performed on the Larmor diffractometer (ISIS, Harwell, UK), with a polychromatic λ=0.9-13.3 Å unpolarised and divergent incident beam with sample-to-detector distance = 4.1 m, yielding a fixed momentum transfer range of approximately $0.005 < Q < 0.6$ Å^{-1} with the peak flux in the intermediate Q range. Quartz cells (1 mm banjo, Starna) containing the surfactant solutions were installed into a metallic sample changer that was thermally controlled using a liquid bath. Experiments were started at 60 °C, where all solutions were in the isotropic micellar phase, and then a variety of cooling ramps were imposed to reach 0 °C.[39] The resulting SANS data were reduced, using standard procedures, in MANTID.[40] Reduced data from Larmor were fitted in SASView (V4.1.2) using an ellipsoidal core-shell model for the form factor and the Hayter-Penfold Rescaled Mean Spherical Approximation (RMSA) to model the structure factor. Due to the expected large contribution of the structure factor at high micellar concentrations studied here, self-consistency checks controlling the volume of surfactant, Scattering Length Densities and ensuring continuous trends in charge, dimensions and structure modifications were performed for all analyses presented here across a wide range of temperature and concentrations.[41, 42]

FTIR spectroscopy. FTIR spectra were recorded in Attenuated Total Reflectance (ATR) mode using a Bruker Tensor 27 System with a Platinum ATR accessory. For each spectrum, 64 single beam scans were averaged with 4 cm^{-1} resolution in the range of 4000 to 600 cm^{-1}. Results were examined in the absorbance unit using OPUS 8.5 software. Standard baseline correction was performed on all the spectra analysed with no further data processing.

Viscosity measurements. Viscosity measurements were performed in a thermally controlled concentric cylinder setup of a Rheometer (AntonPaar MCR302). All tests were started by stabilising the solution at $T = 60$ °C. Cooling measurements were started by stabilising the solution at the temperature of interest for 3 minutes and measuring the viscosity over a range of shear rates

($1\ s^{-1} < \dot{\gamma} < 2000\ s^{-1}$). Zero-shear viscosity of the solutions was extrapolated from the viscosity vs. shear-rate curves by averaging the data in the low shear rate region as they reached a plateau.

3. Results and discussion

We first report our findings on the micellar structures in pure aqueous solutions of SDS and DDAO. Mixed SDS/DDAO systems were then prepared by increasing the concentration of DDAO in SDS solutions of 20 wt% until the onset of the micellar to liquid crystalline phase transitions was detected, see Fig. 1. Primary phase boundaries of the micellar phase in both pure and mixed systems, in the range of temperature tested here ($T < 60$ °C), were identified by means of DLS and OM, whilst structural analyses of the micelles were carried out using SANS and FTIR. Findings on the volumetric concentration, shape and size of the micelles are then used to describe trends found for zero-shear viscosity of solution as a function of composition at various temperatures (ranging from 60 °C down to 0 °C).

3.1. Sodium Dodecyl Sulfate, SDS

DLS analysis of 20 wt% SDS solutions show a fairly mono-disperse (micellar) population whose size gradually increases as temperature decreases. Upon reaching temperatures below 14 °C, a secondary population of larger fast-growing objects, characterised by a slower decay of the auto correlation function, appears which corresponds to the onset of crystallisation in the solution (Fig. 2a). Additionally, nucleation and growth of SDS crystals in solutions of 20 wt% SDS, at temperatures below 14 °C, was clearly detected in OM experiments, shown in the inset images in Fig. 2a. These, preliminary findings from DLS and OM are used as guidelines in defining the temperature range for SANS measurements of the micellar structures during cooling experiments.

SANS experiments upon cooling of 20 wt% SDS solutions were performed between 60 and 0 °C at the rate of $\simeq 0.1$ °C/min. In line with the findings from our DLS and OM analyses, SANS data of pure SDS aqueous solutions at temperatures above 14 °C exhibit one single broad intensity peak in the intermediate-Q region, which is associated with the structure factor of charged SDS micelles.[43, 41] Upon cooling, the intermediate-Q peak increases in intensity whilst moving towards lower Q values (Fig. 2b). Below 14 °C, formation of SDS crystals in the solution leads to the simultaneous appearance of a sharp Bragg peak at $Q \approx 0.2$ Å^{-1} and an upturn in the low-Q region (Fig. 2b). The location of the Bragg peak corresponds to the average d-spacing (about 32-33 Å) between surfactant-rich and water-rich layers in hydrated crystals of SDS.[41]

We next focus on the effect of cooling on micellar solutions of 20 wt% SDS above the crystallisation temperature. The intermediate micellar peak is best fit by the core-shell prolate ellipsoidal model, see Fig. 2c. Prolate ellipsoids were found to systematically provide a better self-consistent fit to our data when compare to oblate ellipsoids. The scattering length densities SLD of the

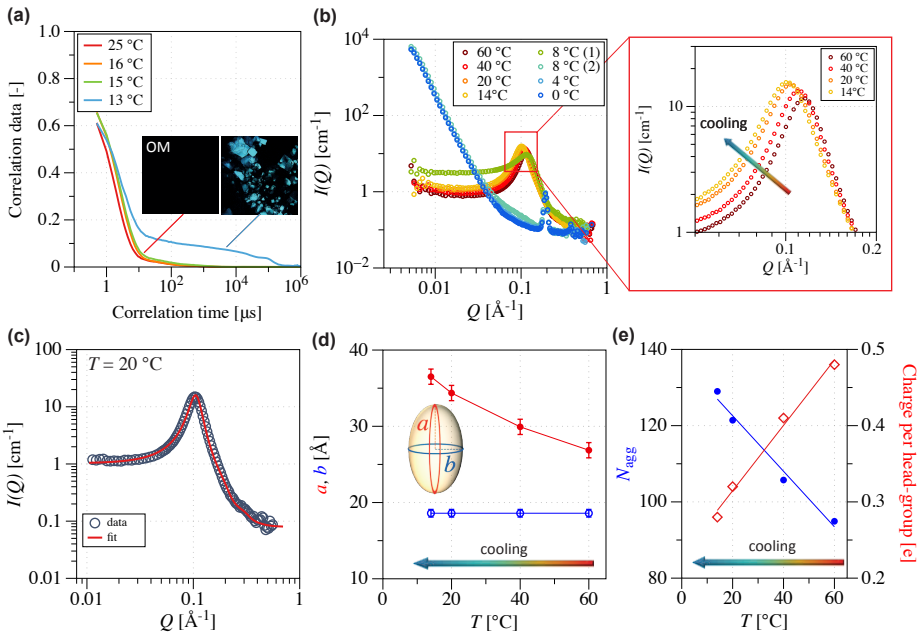

Figure 2: Effect of cooling on 20 wt% SDS aqueous solutions. During a cooling cycle, SDS solutions remain in the micellar phase until reaching temperatures below $T \simeq 14°C$. (a) DLS measurements show the appearance of fast-growing larger objects with long decay times, in addition to the primary micelles, as the solution is cooled down to $T = 13°C$. OM images confirm the isotropic micellar phase at higher temperature $T \geq 14°C$ and the mixed micellar and crystalline phase at $T = 13$ °C (inset). (b) SANS measurements of micellar SDS solutions show a shift in the mid-Q micellar peak towards lower Q values upon cooling. For $T < 14°C$, the micellar peak gradually disappears as a Bragg peak at high-Q and upturn at low-Q, both associated with the crystallisation of SDS, are detected. $T = 8°C$ (1) and $T = 8°C$ (2) correspond to the data acquired at early time (first 3 min) and late time (3-6 min) from the start of experiment at $T = 8°C$, respectively. (c) Illustrative SANS data of SDS micellar phase at 20 °C fitted to a core-shell ellipsoidal model. (d) Prolate micelles of major axis a and minor axis b were found to elongate as the solution is cooled from 60 °C to 14 °C. a increases monotonically upon cooling, while b remains unchanged. (e) Comparatively larger micelles with larger aggregation numbers are obtained upon cooling. The net charge per head-group of SDS molecules (calculated by dividing the fitted total net charge over the aggregation number) also decreases with decreasing temperature.

sodium sulfate shell and dodecyl core of the SDS micelles were calculated and set at fixed values of 4×10^{-6} Å^{-2} and -0.37×10^{-6} Å^{-2}, respectively.[41, 44] Prolate ellipsoidal micelles are defined by the major axis a and the minor axis b. Upon cooling aqueous solutions of SDS at a fixed concentration, the minor axis of the ellipsoid b remains unchanged, while the major axis a grows significantly (Fig. 2d).[45] The prolate ellipsoidal micelles become more elongated upon cooling illustrated through their axial ratio (a/b) increasing from around 1.4 at 60 °C to 2 at 14 °C, before SDS crystallisation begins and consumes the micellar phase.[45] Considering the SDS molecules to occupy an average volume of 410 Å^3 and the volume of the ellipsoidal micelles to be solely occupied by these molecules, the aggregation number (N_{agg}) of SDS micelles can be estimated to increase from $\simeq$95 at 60 °C to $\simeq$130 at 14 °C. These findings, summarized in Fig. 2e, are in agreement (about 5% larger) with values reported by Hammouda.[41] Both axial ratio and the aggregation number of micelles are expected to decrease for lower concentrations of SDS. [31] The overall net charge per micelle slightly decreases at lower temperatures, thus resulting in significantly lower charge per head-group of SDS molecules at lower temperatures, where aggregation numbers are considerably larger (Fig. 2e). In the range of temperatures studied here, the average micellar volume fraction is very close to the volumetric fraction of the surfactant in the solutions, considering an average density of 1.01 g/cm^3 for SDS. These trends are also consistent with previous work by Hammouda [41] for aqueous solutions of 20 wt% of SDS in the temperature range of 20 °C $< T <$ 80 °C.

3.2. Dimethyldodecyl Amine Oxide DDAO

SANS analyses of aqueous solutions of DDAO were carried out for a large range of concentrations (1-30 wt%) and temperatures (4 °C $< T <$ 60 °C), since their effect on DDAO micelles has not been previously reported. Within this parameter space, pure DDAO solutions always remained in the micellar phase during the cooling cycles. Examples of SANS data obtained at various concentrations of DDAO are presented in Fig. 3a. At higher concentrations (above 5 wt%) a clear peak appears in the intermediate-Q range, characteristic of the structure factor of charged micelles. This feature is, however, not present in SANS measurements acquired at lower concentrations of DDAO (Fig. 3a).

The SANS intensity $I(Q)$ of the micellar solutions is the product of the volumetric concentration of the micelles ϕ, contrast factor $\Delta\rho$ and form $P(Q)$ and structure factor $S(Q)$ of the system:

$$I(Q) = \phi V_m (\Delta\rho)^2 P(Q) S(Q) + BG, \tag{1}$$

where $\Delta\rho$ is scattering length density difference between the micelle and the surrounding solvent, V_m is the volume of the micelle and BG is the background intensity. In order to eliminate the effect of the (mostly incoherent) background BG and volumetric concentration of the micelles ϕ, it is customary to rescale the scattering intensity of SANS measurements with concentration ϕ of DDAO to obtain the $(I - BG)/\phi$, as presented in Fig. 3b. The form factor $P(Q)$ for

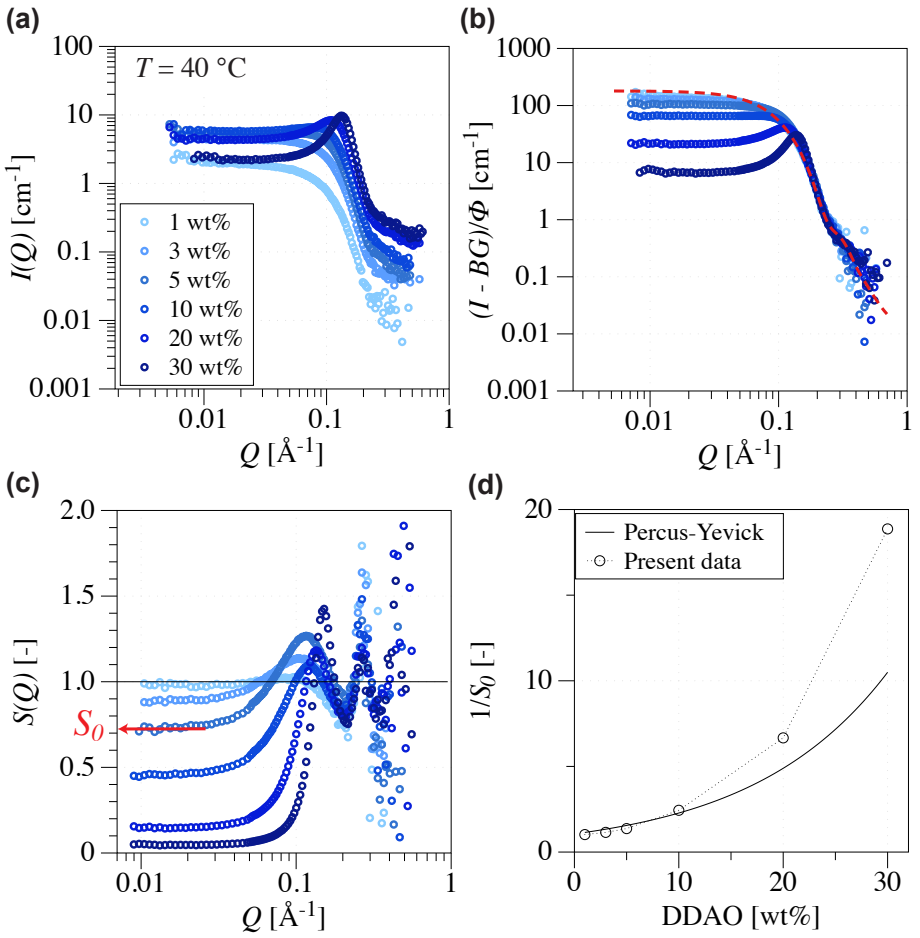

Figure 3: Analyses of SANS data for increasing concentration of DDAO at fixed $T = 40$ °C. (a) As the concentration of DDAO increases above 5 wt%, an intermediate-Q peak appears in the SANS data. (b) Contributions from the background intensity (BG) and the volumetric concentration (ϕ) are eliminated by rescaling the scattered intensity, thus yielding, for sufficiently dilute systems, the form factor $P(Q)$ of the micelles as a function of Q. The dashed red curve represents the term $V_m(\Delta\rho)^2 P(Q)$ calculated based on the form factor estimated for the lowest concentration of DDAO (at 1 wt%). (c) Dividing the SANS intensities by $V_m(\Delta\rho)^2 P(Q)$ provides an estimation of the structure factor for the micellar solutions. The structure factor at $Q \to 0$, denoted as S_0, is used to estimate the osmotic compressibility of the colloidal system. (d) Measurements of $1/S_0$, obtained from the SANS data for increasing concentration of DDAO (open circles), are compared with those calculated using the Percus-Yevick closure (solid line) for hard spheres.

DDAO micelles was estimated for the most dilute solution (at 1 wt%), where $S(Q)$ is not prevalent. The corresponding $V_m(\Delta\rho)^2 P(Q)$ term is depicted by a red dashed curve in Fig. 3b. We then calculate the structure factor $S(Q)$ for the micellar solutions of DDAO at various concentrations by simply dividing the corresponding SANS intensities by $V_m(\Delta\rho)^2 P(Q)$, see Fig. 3c. This procedure allows for quantification of the structure factor at zero scattering angle S_0 and consequently estimation of the osmotic compressibility of the system (e.g. [44, 46]). Fig. 3d shows the comparison between calculated values of $1/S_0$ from the present SANS data and those estimated considering the Percus-Yevick closure for hard spheres, S_{PY}:

$$S_{\mathrm{PY}} = \frac{(1-\phi)^4}{(1+2\phi)^2}. \tag{2}$$

The relatively larger deviation for higher concentration of DDAO (> 5 wt%), indicates that other sources of interaction between the micelles must be considered when modelling micellar solutions of higher concentrations of DDAO. Here, the Rescaled Mean Spherical Approximation RMSA is used to model the structure factor for all solutions of DDAO and considering the intra-micellar interaction as Coulombic repulsion.[42, 47]

The best fits to SANS data of aqueous solutions of C_{12}AO across the entire range of temperatures and concentrations were obtained using a prolate ellipsoidal core-shell model (Fig. 4a).[36, 48] The scattering length densities SLD for the dimethyl amine oxide shell and the dodecyl core of DDAO micelles were taken as 0.76×10^{-6} Å^{-2} and -0.37×10^{-6} Å^{-2}, respectively.[36] Increasing concentration of DDAO induced minor elongation in the prolate ellipsoidal micelles (Fig. 4b). The axial ratio of the micelles increased from around $a/b = 1.7$ to $a/b = 1.9$. DDAO micelles were also found to carry small amount of net charge, especially at higher concentrations of surfactant, resulting in a repulsive interaction between the micelles.[36] The increase in the net charge of micelles is believed to correspond to the protonation of the head group of DDAO molecules which leads to a slight increase in the pH of the solution at higher DDAO concentrations (Fig. 4c).[49, 28] This fitted net charge per DDAO micelles becomes significant only at concentrations above 5 wt% of DDAO, in agreement with conclusions based on estimation of compressibility of the micellar solutions reported in Fig. 3d. The net charge per head-group of DDAO is estimated to be around 0.1 for 20 wt% DDAO, using the fitted values obtained for the aggregation number of micelles. This value is in good agreement with previous reports in the literature.[36] Overall, unlike in SDS solutions, the size and shape of DDAO micelles remain relatively invariant upon cooling, as shown in the SANS data in Fig. 4d,e for solutions of 3 and 30 wt% of DDAO as a function of temperature. This likely reflects the difference in inter- and intra-micellar interactions in anionic and non-ionic surfactant solutions. In anionic surfactant solutions, the size, shape and inter-micellar interactions are dominated by electrostatic interactions between charged head groups and counterions. At lower temperatures, much like for cationic surfactants,[50] counterion binding increases and

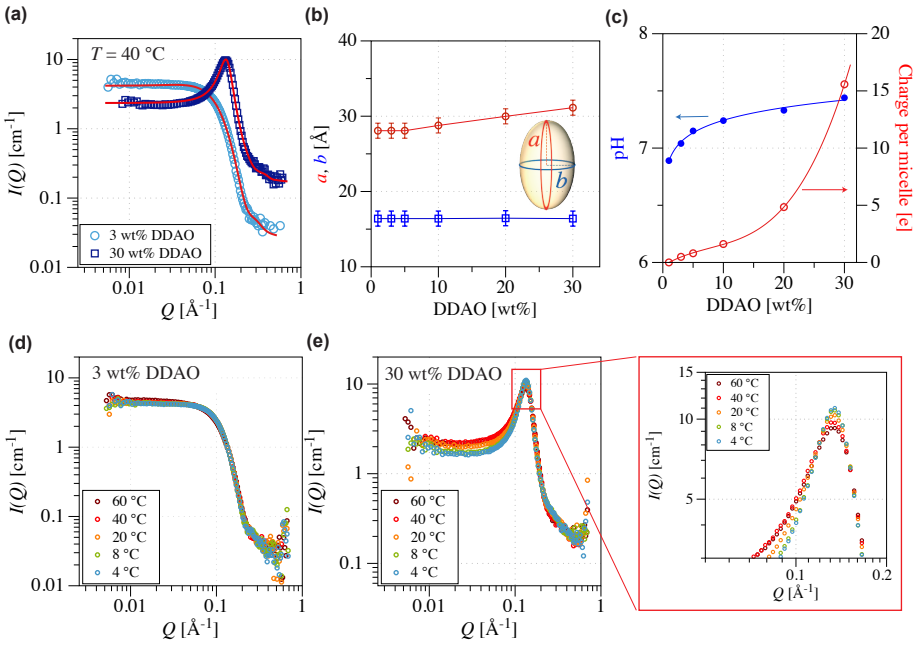

Figure 4: SANS measurements for aqueous solutions of DDAO at different concentrations and temperatures. (a) The best fits to aqueous micellar solutions of DDAO are obtained using the prolate core-shell ellipsoidal model as the form factor and the for the structure factor. Examples of typical fits for DDAO solutions at 3 and 30 wt% at $T = 40$ °C. (b) The major axis of the ellipsoidal micelles a decreases with increasing DDAO concentration, while the minor axis b remains broadly unchanged. (c) The fitted net charge per surfactant head-group increases as the concentration of DDAO increases. Additionally, the pH of the solution slightly increases to reach values about 7.5 for solutions of highest concentration of DDAO. SANS data at 3 wt% (d) and 30 wt% (e) of DDAO acquired in cooling experiments. (d) The SANS profiles remain fairly unchanged at lower concentrations of DDAO. (e) At higher concentrations of DDAO, the intensity of the mid-Q micellar peak increases in intensity at lower temperatures, however, its position remains constant.

screens head-group repulsion and allows micelles to swell (predominantly in the axial direction). For the non-ionic (or minimally charged) DDAO micelles, no such ionic effect is prevalent and changes in temperature appear to have minimal effect on the hydration of head-group and packing of the tails and therefore do not affect the micelle size or shape.

In order to examine the packing and interaction of the amine oxide head-groups and its relation to the shape of the DDAO micelles, we perform FTIR measurements (Fig. 5). To monitor the protonation of the head-group and the elongation of the micelles of DDAO, we focus on the frequency bands at 1180-1280 cm^{-1} and 2800-2950 cm^{-1}, respectively.[22, 51] The significant increase in the relative intensity of peak located at about 1195 cm^{-1} for higher concentrations of DDAO in Fig. 5a, which is associated with the ionic character of the N-O link, has been previously reported to be linked to the protonation of the

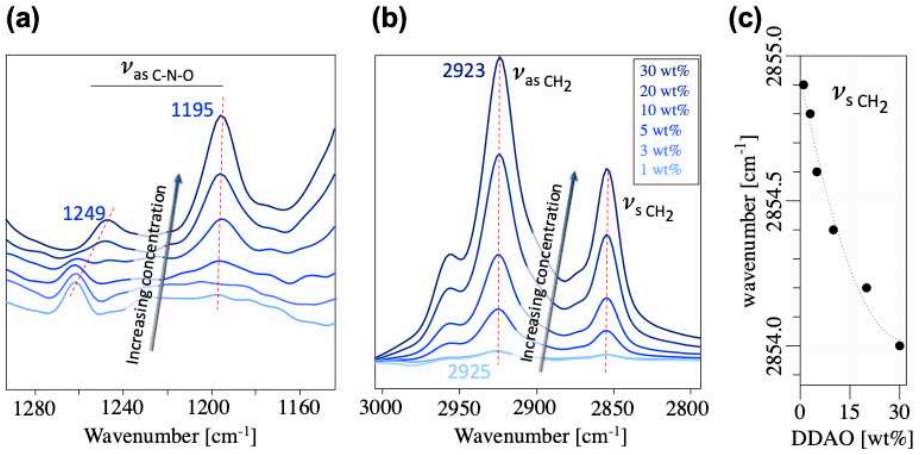

Figure 5: ATR-FTIR spectra of aqueous solutions of pure DDAO for various concentrations (1-30 wt%) at $T = 20$ °C: (a) antisymmetric C-N-O stretching region (around ν_{as} C-N-O). The relative intensity of the peak at 1195 cm^{-1} increases significantly as DDAO concentration is increased. (b) C-H stretching region. The symmetric stretching band is often used to monitor the ordering of the hydrocarbons in tail-group of the surfactant molecules. (c) The symmetric CH_2 peak shifts subtly towards lower wavenumbers indicating a higher level ordering in the tail groups.

head-group in the DDAO molecules.[15] This observation confirms the increase in net charge of the DDAO and corresponding increase in the pH of the solution found from fitting SANS data, see Fig. 4c. Both symmetric (at around 2850 cm^{-1}) and antisymmetric (at around 2920 cm^{-1}) IR absorption bands of CH_2 can be used as indicators for tracking the tail-group ordering. However, since the antisymmetric band also contains contributions from the CH_3 group, here we mainly focus on the symmetric CH_2 band to monitor elongation of micelles.[52] Upon increasing the concentration of DDAO, a continuous shift towards lower frequencies (from 2855 cm^{-1} to 2854 cm^{-1}) is observed in the location of the symmetric CH_2 peak, suggesting an increase in the ordering of the tail groups within the micelles (Fig. 5b).[22] We associate this effect to the formation of more elongated objects that is in agreement with observation of slightly more stretched ellipsoidal micelles at higher concentrations of DDAO, see Fig. 4b.

3.3. Mixed SDS/DDAO systems

Our main goal here is to investigate the effect of cooling and increasing concentration of DDAO on SDS micelles. We focus on mixed SDS/DDAO systems comprising a fixed concentration of 20 wt% SDS and varying concentration of DDAO. Since no pure micellar phase was found for solutions with more than 5 wt% DDAO, in the range 0-60 °C (Fig. 1), our SANS and FTIR measurements were bounded to this limit. In general, the regions to the right and below the phase boundaries in Fig. 1(right side) were composed of coexisting L_1+LC and L_1+C and LC+C phases, which will be examined in a separate publication.

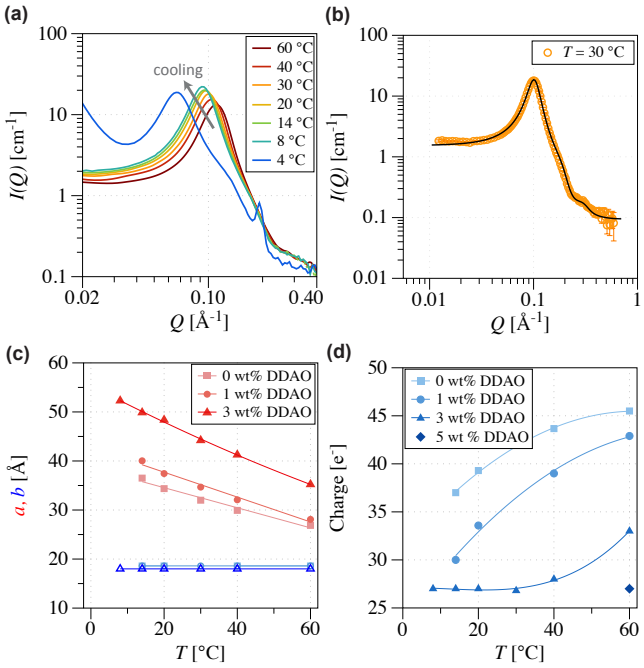

Figure 6: Effect of cooling on mixed SDS/DDAO micelles. (a) Example of SANS measurements in the intermediate-Q region for an aqueous solution of 20 wt% SDS and 3 wt% DDAO in a cooling cycle. Upon cooling the solution below 8 °C, the micellar phase coexists with the crystalline phase, marked by the simultaneous appearance of a sharp Bragg peak and an upturn in the low-Q region. (b) An example of a core-shell prolate ellipsoidal model fit to the SANS data acquired for aqueous solution of 20 wt% SDS and 3 wt% DDAO at $T = 30$ °C. (c) For all solutions, the major axis of the ellipsoids a elongates upon cooling, while the minor axis b remains unchanged. Consequently, the axial ratio a/b increases from 1.5 for pure SDS solutions at the highest temperature to about 3 for mixed solutions at the lowest temperatures of interest. (d) The net charge carries by mixed micelles decreases at lower temperatures and higher DDAO concentrations.

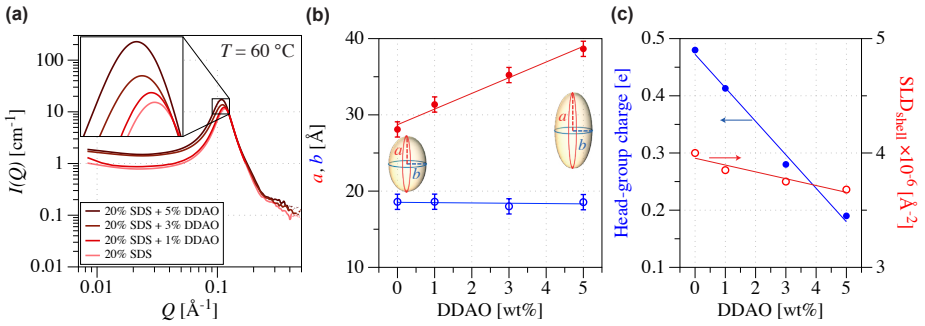

Figure 7: Effect of increasing concentration of DDAO on the structure of mixed SDS/DDAO micelles at a fixed temperature ($T = 60$ °C). (a) SANS data show a clear shift in intensity and position of the (intermediate-Q) micellar peak. (b) Mixed micelles are well described by a core-shell prolate ellipsoidal model, and DDAO addition is found to elongates the major axis (a) of the ellipsoidal micelles, while the minor axis (b) remains nearly unchanged. (c) The fitted net charge of the mixed micelles decreases upon increasing DDAO content. Incorporation of DDAO into SDS micelles reduces the fitted the SLD of the shell associated to the formation of mixed micelles. The x-axes in (b) and (c) represent the concentration of DDAO added to solutions with a fixed concentration of SDS (20 wt% in the final mixture).

Fig. 6a exhibits an example of SANS data obtained in a cooling experiment for a mixed SDS/DDAO solution, initially in the micellar region. Similar to the pure SDS solutions, a transition form the pure micellar (L_1) to the mixed micellar/crystalline phase (L_1+C) is detected for the solution of 20 wt% SDS + 3 wt% DDAO, although at relatively lower temperature. In the micellar phase, lowering the temperature shifts the L_1 peak at intermediate-Q towards lower-Q values, similar to the trend observed for pure SDS micelles. Best fits to the SANS data of mixed SDS/DDAO micelles were found using prolate core-shell ellipsoidal models (Fig. 6b). The major axis of the micelles was found to considerably grow in length, upon decreasing temperature. The length of the minor axis remains fairly unchanged at all temperatures and compositions, attributed to the fact that this is predominantly fixed by the tail length of the surfactants which are nominally the same for SDS and DDAO here (Fig. 6c). Consequently, the ellipsoidal micelles elongate and their axial ratio a/b increases from around 1.5 to 3 as the solutions are brought to lower temperatures. The elongation of the ellipsoidal micelle is amplified with higher DDAO content due to molecular interactions that will be rationalised by FTIR analyses (Fig. 8). As pure and mixed micelles of SDS and DDAO become more ellipsoidal upon cooling, the net charge on the micelles decreases, thus resulting in less electrostatic repulsion between the aggregates (Fig. 6d). The aggregation number of the mixed micelles increases monotonically with increasing total surfactant concentration and decreasing temperature, similar to the trends reported for aqueous solutions of SDS.[53, 54, 41]

At a fixed temperature, in the region where all solutions are in the micellar phase ($T = 60$ °C), increasing the concentration of DDAO shifts the intermediate-Q micellar peak towards lower Q values, indicative of a reduced

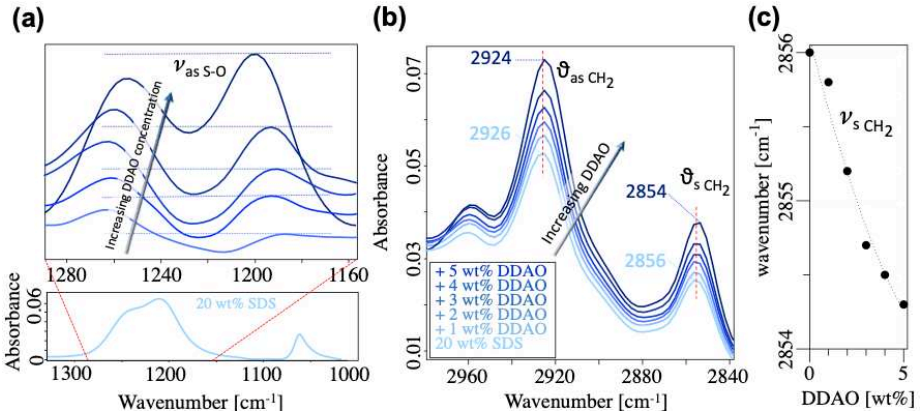

Figure 8: ATR-FTIR spectra of mixed SDS/DDAO micellar solutions at $T = 20$ °C. (a) S-O stretching region of sulfate head-group in SDS/DDAO mixed micelles. In each case, the spectrum of pure SDS at 20 wt% (in light blue) is subtracted from the spectrum of mixed SDS/DDAO solutions. (b) The C-H stretching region of pure SDS solutions (20 wt%) and mixtures of 20 wt% SDS with varying amounts of DDAO, ranging from 1 to 5 wt%. (c) The frequency of the symmetric C-H stretching is used to monitor the ordering of the tail-groups in the mixed micelles.

spatial extent of repulsive interaction between charged objects (Fig. 7a). These trends translate into the elongation of prolate ellipsoidal micelles upon addition of DDAO (Fig. 7b). As more DDAO molecules are incorporated within the micelles, the net charge per head-group of surfactants is significantly reduced (Fig. 7c), thus allowing surfactant molecules to pack more efficiently and adopt more elongated structures.

Furthermore, increasing the concentration of DDAO in mixed micelles causes the overall fitted scattering length density of the micelles to drop to lower values (Fig. 7c). Scattering length densities of head-groups in SDS and DDAO are taken to be $\simeq$4 and 0.76, respectively, and therefore, a reduction in SLD values upon DDAO addition further corroborates the formation of mixed micelles.

Infrared spectroscopy analysis of mixed SDS/DDAO systems is used to examine the head-group interactions between the two surfactants and ordering of the tail-groups (Fig. 8). Comparison between the spectra of neat SDS solutions and those of mixed micelles in the fingerprint region can elucidate the interactions between SDS and DDAO head-groups. Fig. 8a shows a reference SDS micellar spectrum and series of difference spectra of SDS/DDAO mixed micellar solutions in the frequency range which depicts the anti-symmetric S-O stretching bands of the SDS head-groups. In general, three bands are assigned to the sulfate head-group vibrations of SDS molecule. Two are considered to be generated due to S-O asymmetric stretching vibrations ($\nu_{\mathrm{as\ S-O}}$ at 1215 and 1210 cm^{-1}) and the third due to symmetric vibrations ($\nu_{\mathrm{s\ S-O}}$ at 1060 cm^{-1}). Interpretation of the spectral changes of SDS head-group, in terms of mixed micelle structure, requires understanding of how these bands respond to changes in their local environment. The transition dipole moment of $\nu_{\mathrm{as\ S-O}}$ is located along the

micelle surface and that of $\nu_{s\ S-O}$ is located in the direction normal to micelle surface. Several detailed solution studies of mixed SDS micelles attributed the shift and splitting of $\nu_{as\ S-O}$ band to the lateral interactions of S-O bond.[22] Consistent with those results, a constant $\nu_{s\ S-O}$ band in our study shows that the interaction may not involve any component normal to the surface. Furthermore, the observation of the splitting and shifting of $\nu_{as\ S-O}$ band, which might result from a reduction in the symmetry of sulfate head-group, suggests lateral electrostatic interactions between SDS and DDAO molecules. Since the lateral interaction between SDS and DDAO affects the overall micellar structure, the surfactant tail-groups must spatially rearrange to accommodate the reduction in head-group area. The regions associated with the symmetric and antisymmetric vibrations of CH_2 in the tail-groups are presented in Fig. 8b. In the spectra of the mixtures, the two major bands near 2925 cm^{-1} (asymmetric CH_2 stretch) and 2854 cm^{-1} (symmetric CH_2 stretch) are composites, due to the extensive overlap of these bands in the spectra of the individual surfactants. The CH_2 stretching band frequency exhibits a concentration dependent decrease as the DDAO content increases in the system, Fig. 8c. The frequency decrease suggests a decrease in the gauche/trans conformer ratio of the surfactant tails, *i.e.*, an increase in the ordering of the tails in the mixed micelles.[52] This observation is in line with formation of more elongated prolate ellipsoid found from our SANS measurements.

3.4. Viscosity of mixed micellar solutions

The effect of micelle shape and volumetric concentration on the rheological behaviour of mixed surfactant solutions has been previously studied in detail in the context of dramatic transformations from spherical to cylindrical and worm-like structures. [22, 55, 56, 57, 14, 24] Comparatively fewer investigations have considered the effect of gradual and modest shape changes in micelles, from spherical to prolate/oblate ellipsoids, on solution viscosity. For colloidal solutions of solid particles, the aspect ratio of anisometric particles is a critical variable defining the complex rheological behaviour of particle-bearing liquids, especially at higher concentrations. In general, increasing particle anisometry significantly decreases the critical jamming concentration of the solution, at a given volumetric colloidal concentration, and increases the apparent fluid viscosity for solutions with mild shear-thinning behaviour.[58, 59, 60] Such effects are attributed to the enhanced orientability and particle-particle interactions in solutions of anisometric particles. Here, we explore the effect of temperature and composition of the SDS/DDAO solutions, where gradual spherical-prolate ellipsoid transitions are observed in our SANS and FTIR measurements, on their rheological behaviour. Significantly, this transformation occur at nearly-constant micellar volume fraction (or number density) thereby providing a suitable model system for this study.

Generally, the mixed SDS/DDAO solutions of interest are considerably more viscous than pure SDS solutions, at similar total surfactant concentration. Fig. 9 presents zero-shear viscosity measurements at different temperatures and surfactant concentrations. All solutions with 20 wt% SDS and 0-3 wt% of added

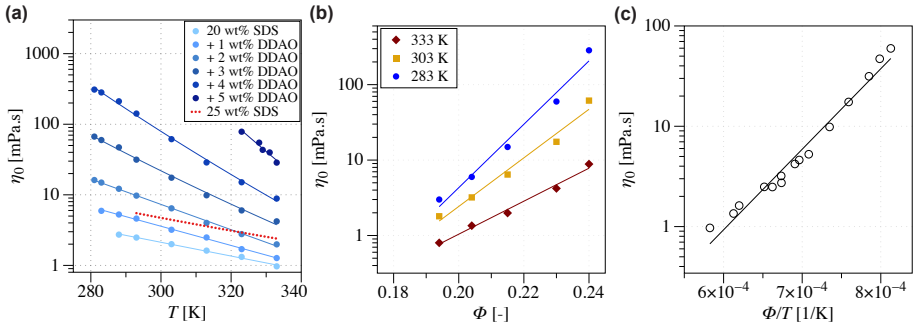

Figure 9: Effect of cooling and DDAO composition on the viscosity of mixed SDS/DDAO micellar solutions: (a) Zero-shear viscosity η_0 of aqueous micellar solutions of pure SDS and mixed SDS/DDAO as a function of temperature, showing an exponential increase (by more than one order of magnitude) with decreasing temperature, which is magnified at higher concentrations of DDAO. Viscosity measurements for pure SDS solutions at 20 wt% and 25 wt% (red dashed line) are provided for comparison. (b) Viscosity of micellar solutions increases exponentially with increasing concentration of DDAO and total concentration of the surfactant in the solution, and this trend holds at different temperatures within the micellar region of the phase map. The x-axis represents the volumetric concentration of micelles (ϕ) obtained from model fits to the SANS data. (c) A single reduced variable ϕ/T is found to collapse all the zero-shear viscosity data of the solutions investigated, within measurement uncertainty.

DDAO exhibited Newtonian behaviour in the parameter space studied here. Solutions with 4 wt% DDAO showed mild shear thinning behaviour at higher shear rates (> 100 s^{-1}) and lower temperatures. For both pure SDS and mixed SDS/DDAO systems, zero-shear viscosity increases exponentially with decreasing temperature, given here as absolute temperature (in K). Cooling from 60 °C to 20 °C, causes the viscosity of pure SDS solutions to increase by approximately 3 fold. This trend is similar to that obtained when cooling the pure solvent (water), even though SDS solutions are typically more viscous than water. However, a similar reduction of temperature causes more than 10 fold increase in viscosity of the mixed SDS/DDAO solutions (Fig. 9a). The significant difference between the viscosity of micellar solutions of mixed SDS/DDAO and pure SDS, with identical total surfactant concentrations, shows that even moderate modification of micelle composition and shape leads to considerable changes in the bulk properties of the solutions. Similarly, the viscosity of mixed SDS/DDAO micellar solutions increases exponentially with increasing the DDAO concentration in a solution with a fixed concentration of 20 wt% SDS. At a fixed temperature, increasing total concentration of surfactant by less than 20%, leads to more than a 10-fold increase in viscosity of the mixed systems, likely owing to the strong synergistic interaction between the two surfactant and elongation of the micelles (Fig. 9b). Since the viscosity data presented here follow exponential trends with both volume fraction of the surfactant and reciprocal of absolute temperature, a single exponential function based on a new variable, ϕ/T, can be used to collapse all solution viscosity data, shown in Fig. 9c, and thus provides

a simple, albeit empirical, predictive tool.

Based on our SANS measurements, solution composition and temperature largely define the structure and properties of mixed SDS/DDAO micelles. Whilst the combined effect of added DDAO concentration and temperature variations on the intra-micellar interactions is rather complex, we find a simple monotonic trend between these two variables and the geometrical shape of the micelles. In particular, for our system of prolate ellipsoidal micelles, temperature and concentration of DDAO determine the axial ratio of the mixed micelles a/b, see Fig. 10a for a map with contours at constant axial ratios. At high temperature and small amount of DDAO (added to solutions of 20 wt% SDS), the axial ratio of ellipsoidal micelles is close to one (top-left corner of the contour map in Fig. 10a), while axial ratios around $a/b = 3$ are obtained at lower temperature and higher content of DDAO. Based on the findings presented in Fig. 9c that the viscosity of our solutions of interest can be well described by a single variable, namely ϕ/T, we investigate the relationship between this variable and the axial ratio the micelles. Fig. 10b shows that a simple linear function can correlate ϕ/T to values of a/b. Consequently, it is expected that the viscosity of the solutions can be simply related to the axial ratio of the micelles by a single exponential function ($\eta_0 \propto e^{2.8(a/b)}$), see Fig. 10c.

A convenient and commonly used approach to characterise the effect of shape of non-spherical particles on rheological behaviour of colloidal suspensions is through determination of the intrinsic viscosity, defined as:

$$[\eta_0] = \frac{\eta_0 - \eta_s}{\eta_s \phi}, \tag{3}$$

where ϕ is volume fraction of the colloids and η_s is the viscosity of the solvent, see the inset in Fig. 10c. The impact of colloidal shape, especially aspect ratio of elongated colloids on the intrinsic viscosity of Brownian suspensions, has been extensively investigated through analytical and numerical methods. Classic predictions of intrinsic viscosity for prolate Brownian rigid colloidal suspensions are compared to those obtained for our current surfactant micellar solutions in Fig. 10d as a function of aspect ratio of the particles.[61, 62] Interestingly, current measurements of intrinsic viscosity of mixed micellar solutions are up to two orders of magnitude larger than theoretical predictions for Brownian suspensions. Considering that solution viscosity is enhanced at higher content of DDAO and lower temperature at which the intra-micellar electrostatic repulsive interaction is significantly reduced compared to pure SDS solutions of similar concentrations, we speculate the effect to be caused by the appearance of local anisotropic domains within the micellar solution under shear. Increased surfactant concentration and alignment of ellipsoidal micelles within these domains may promote local phase transformation to liquid crystals that is expected for higher concentration of DDAO at lower temperature. Note that the increase in the absolute viscosity values (10^{-3} to 10^{-1} Pa.s) for our concentrated solutions of elongated micelles reported in Fig. 10c, although significant, is much lower than that expected for transformations from globular to worm-like micelles in similar systems which is typically on the order (10^{-3} to 10^{5} Pa.s),[63, 64, 65]

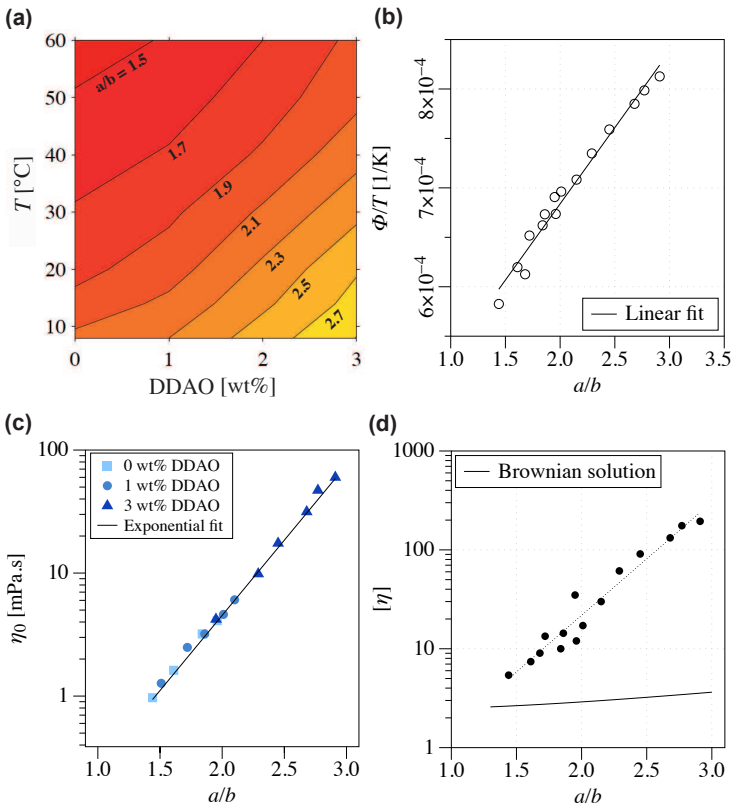

Figure 10: Effect of micelle shape on the viscosity of mixed micellar solutions. (a) Temperature-concentration map of contours with constant axial ratios (a/b) of mixed SDS/DDAO ellipsoidal micelles. Values of a/b were extracted from fits to the corresponding SANS data. The x-axis represents the concentration of DDAO added to a solutions of 20 wt% SDS. (b) The combined variable ϕ/T presented in Fig. 10c is found to depend linearly on the micellar aspect ratio a/b. (c) Viscosity of mixed SDS/DDAO solutions can be predicted by an exponential function ($\propto e^{2.8x}$) of a single variable, namely the axial ratio of ellipsoidal micelles (a/b). The axial ratio of micelles is a dependent variable that is defined by independent variables T and DDAO concentration. (d) Intrinsic viscosity of the present micellar solutions vs. the aspect ratio of the micelles. The prediction model from Brenner [61] for Brownian colloidal suspensions is illustrated by a solid black line for comparison.

therefore, it cannot be attributed to such dramatic transformation. Rational interpretation of the relatively significant viscosity increase observed here requires further under-shear scattering and/or (electron)microscopy measurements.

4. Conclusion

We have systematically investigated the effect of cooling in the wide range of 60 °C down to 0 °C on pure and mixed micellar solutions of SDS and DDAO using complementary experimental tools. In order to relate the molecular scale understanding of our systems to their bulk properties, we combined inter- and intra-micellar structural analyses through SANS and FTIR measurements, alongside zero-shear viscosity measurements.

In pure SDS solutions, decreasing the temperature causes micellar elongation, in agreement with previously reported trends at higher temperatures.[41] Both SANS and FTIR measurements suggest that pure DDAO micelles carry a net charge due to the protonation of the head-group especially at higher concentrations (above 5 wt%). We then analysed mixed solutions of 20 wt% SDS and varying DDAO content. No pure micellar phase existed within our current range of temperatures for DDAO concentrations above 5 wt%, therefore, SANS and FTIR measurements were focused on this composition range.[22] We confirmed the formation of mixed micelles by monitoring the interactions between the SDS and DDAO head-groups using SANS and FTIR measurements. Incorporation of DDAO into SDS micelles was found to decrease the net charge of the micelles, reducing the area designated to the surfactant head-group and consequently increasing the packing parameter. In turn, mixed SDS/DDAO prolate ellipsoidal micelles are found to be more elongated than neat solutions of either surfactant.[31] This finding is in general agreement with observations reported for other mixed SDS/DDAO solutions of different composition and concentrations. In parallel to the findings from SANS measurements, elongation of the ellipsoidal micelles is clearly accompanied by the decreasing frequency of the symmetric C-H bond with FTIR, analogous to those observed during spherical-to-rodlike transitions.[52, 22] Moreover, head-group interactions between SDS and DDAO were captured by monitoring the FTIR spectral bands of the sulfate groups in mixed micellar solutions.

Detailed zero-shear viscosity measurements for mixed SDS/DDAO solutions at various compositions and temperatures characterised bulk solution properties which we sought to link to molecular structure. Mixed solutions were found to be significantly more viscous than pure SDS solutions at identical surfactant concentration. We found exponential trends between viscosity of the solution and both temperature and volume fraction of the micellar phase, and empirically found that a single combined variable, namely ϕ/T, can be used to estimate the viscosity of the solutions in the experimental range studied. Based on our SANS measurements, we obtained a contour map of micellar shape, and specifically aspect ratio of the micelles, as a function of the temperature and DDAO content in the solution. We found the variable ϕ/T to be a linear function of the micellar aspect ratio, thus allowing for the viscosity of the solutions to be instead

predicted by a single exponential function of aspect ratio. We suggest that this approach may be more widely applicable to other soft, anisometric particulate systems. We highlighted the effect of micellar size and shape on the viscosity of the solution by considering the intrinsic viscosity. Compared to classic models for intrinsic viscosity prediction in suspensions of prolate ellipsoidal colloids, mixed SDS/DDAO micelles are significantly more viscous.[61]

Complementary to common expectation in the surfactant literature that significant viscosity increases (up to 5-6 orders of magnitude) in the micellar solutions are often linked to dramatic spherical-to-wormlike or rodlike shape transitions, here we report changes in micellar solution viscosity of up to 2-3 orders of magnitude that are associated with comparatively modest micellar elongation ($a/b < 10$). The small elongation regime investigated here covers the initial stages of the growth before worm-like micelles are formed. The enhanced viscosity of micellar solutions observed in this regime might be attributed to appearance of anisotropic domains where local fluctuation in concentration and other degrees of freedom may cause phase transformations. Precise validation of this speculation requires further real-time multiscale investigation of these systems under shear.

5. Acknowledgements

We thank the National Formulation Centre (NFC) of the Centre for Process Innovation (CPI, UK), Procter & Gamble and BP-Castrol for funding the microSTAR partnership. Experiments at the ISIS Neutron and Muon Source were supported by a beamtime allocation RB1820374[66] from the Science and Technology Facilities Council. We thank Jack F Douglas (NIST) for discussions on the viscosity of particle and colloidal suspensions. This work benefited from the use of the SasView application, originally developed under NSF Award DMR-0520547. SasView also contains code developed with funding from the EU Horizon 2020 programme under the SINE2020 project Grant No 654000.

[1] F. J., Surfactants in consumer products, Springer, 1987.

[2] C. K. Ahn, Y. M. Kim, S. H. Woo, J. M. Park, Soil washing using various nonionic surfactants and their recovery by selective adsorption with activated carbon, J. Hazard. Mater. 154 (1) (2008) 153–160.

[3] A. Karthick, B. Roy, P. Chattopadhyay, A review on the application of chemical surfactant and surfactant foam for remediation of petroleum oil contaminated soil, J. Environ. Manage. 243 (2019) 187–205.

[4] J. J. Sheng, Status of surfactant EOR technology, Petroleum 1 (2) (2015) 97–105.

[5] C. A. F. Castro M. J. L., Ojeda C., Surfactants in Agriculture. In Green Materials for Energy, Products and Depollution. Environmental Chemistry for a Sustainable World, Vol. 3, Springer, Dordrecht, 2013.

[6] I. Kralova, J. Sjöblom, Surfactants used in food industry: a review, J. Disper. Sci. Technol. 30 (9) (2009) 1363–1383.

[7] D. Myers, Surfactant Science and Technology, Wiley, 2005.

[8] L. L. Schramm, E. N. Stasiuk, D. G. Marangoni, Surfactants and their applications, Annu. Rep. Prog. Chem., Sect. C: Phys. Chem. 99 (2003) 3–48.

[9] B. Kronberg, K. Holmberg, B. Lindman, Mixed surfactant systems, Marcel Dekker, Inc., 1992.

[10] K. Shinoda, The critical micelle concentration of soap mixtures (two-component mixture), J. Phys. Chem. 58 (7) (1954) 541–544.

[11] D. N. Rubingh, Mixed micelle solutions, Vol. 1, Springer New York, Boston, MA, 1979, pp. 337–354.

[12] J. F. Scamehorn (Ed.), Phenomena in mixed surfactant systems, ACS symposium series No. 311, American Chemical Society, 1986.

[13] K. B., Surfactant mixtures, Curr. Opin. Colloid In. 2 (5) (1997) 456 – 463.

[14] B. A. Schubert, E. W. Kaler, N. J. Wagner, The microstructure and rheology of mixed cationic/anionic wormlike micelles, Langmuir 19 (10) (2003) 4079–4089.

[15] J. F. Rathman, J. F. Scamehorn, Counterion binding on mixed micelles, J. Phys. Chem. 88 (24) (1984) 5807–5816.

[16] C. M. Nguyen, J. F. Rathman, J. F. Scamehorn, Thermodynamics of mixed micelle formation, J. Colloid Interf. Sci. 112 (2) (1986) 438 – 446.

[17] J. Penfold, I. Tucker, R. K. Thomas, E. Staples, R. Schuermann, Structure of mixed anionic/nonionic surfactant micelles: experimental observations relating to the role of headgroup electrostatic and steric effects and the effects of added electrolyte, J. Phys. Chem. B 109 (21) (2005) 10760–10770.

[18] R. Abdel-Rahem, Synergism in mixed anionic–amphoteric surfactant solutions: Influence of anionic surfactant chain length, Tenside Surfactants Detergents 46 (5) (2009) 298–305. doi:10.3139/113.110035.

[19] D. Saul, G. J. T. Tiddy, B. A. Wheeler, P. A. Wheeler, E. Willis, Phase structure and rheological properties of a mixed zwitterionic/anionic surfactant system, J. Chem. Soc., Faraday Trans. 1 70 (1974) 163–170.

[20] K. Tsujii, N. Saito, T. Takeuchi, Krafft points of anionic surfactants and their mixtures with special attention to their applicability in hard water, J. Phys. Chem. 84 (18) (1980) 2287–2291.

[21] M. Abe, K. Kato, K. Ogino, Effects of inorganic electrolytes and of ph on micelle formation of amphoteric-anionic mixed surfactant systems, J. Colloid Interf. Sci. 127 (2) (1989) 328 – 335.

[22] J. G. Weers, J. F. Rathman, D. R. Scheuing, Structure/performance relationships in long chain dimethylamine oxide/sodium dodecylsulfate surfactant mixtures, Colloid Polym. Sci. 268 (9) (1990) 832–846.

[23] G. Kume, M. Gallotti, G. Nunes, Review on anionic/cationic surfactant mixtures, J. Surfactants Deterg. 11 (1) (2008) 1–11.

[24] L. Zhang, W. Kang, D. Xu, H. Feng, P. Zhang, Z. Li, Y. Lu, H. Wu, The rheological characteristics for the mixtures of cationic surfactant and anionic–nonionic surfactants: the role of ethylene oxide moieties, RSC Adv. 7 (2017) 13032–13040.

[25] N. Funasaki, S. Hada, Surface tension of aqueous solutions of surfactant mixtures. the composition of mixed micelles, J. Phys. Chem. 83 (19) (1979) 2471–2475.

[26] E. Summerton, M. J. Hollamby, G. Zimbitas, T. Snow, A. J. Smith, J. Sommertune, J. Bettiol, C. Jones, M. M. Britton, S. Bakalis, The impact of N,N-dimethyldodecylamine N-oxide (DDAO) concentration on the crystallisation of sodium dodecyl sulfate (SDS) systems and the resulting changes to crystal structure, shape and the kinetics of crystal growth, J. Colloid Interf. Sci. 527 (2018) 260–266.

[27] J. S. Leal, X. Domingo, F. Comelles, M. T. García, A. Casaña, Interaction of Sodium Dodecyl Sulphate and Dimethyl-Dodecyl-Amine Oxide in aqueous solutions, Springer US, Boston, MA, 1989, pp. 431–441. doi:10.1007/978-1-4615-7984-7_29.
URL https://doi.org/10.1007/978-1-4615-7984-7_29

[28] H. Maeda, R. Kakehashi, Effects of protonation on the thermodynamic properties of alkyl dimethylamine oxides, Adv. Colloid Interface Sci. 88 (1) (2000) 275–293.

[29] M. S. Bakshi, R. Crisantino, R. De Lisi, S. Milioto, Volume and heat capacity of sodium dodecyl sulfate-dodecyldimethylamine oxide mixed micelles, J. Phys. Chem. 97 (26) (1993) 6914–6919.

[30] R. Crisantino, R. De Lisi, S. Milioto, Energetics of sodium dodecyl sulfate-dodecyldimethylamine oxide mixed micelle formation, J. Sol. Chem. 23 (6) (1994) 639–662.

[31] M. Kakitani, T. Imae, M. Furusaka, Investigation of mixed micelles of Dodecyldimethylamine Oxide and Sodium Dodecyl Sulfate by SANS: shape, size, charge, and interaction, J. Phys. Chem. 99 (43) (1995) 16018–16023.

[32] T. P. Goloub, R. J. Pugh, B. V. Zhmud, Micellar interactions in nonionic/ionic mixed surfactant systems, J. Colloid Interf. Sci. 229 (1) (2000) 72–81.

[33] R. Nagarajan, Molecular packing parameter and surfactant self-assembly: the neglected role of the surfactant tail, Langmuir 18 (1) (2002) 31–38.

[34] E. Summerton, M. J. Hollamby, C. S. L. Duff, E. S. Thompson, T. Snow, A. J. Smith, C. Jones, J. Bettiol, S. Bakalis, M. M. Britton, Nuclear magnetic resonance and small-angle X-ray scattering studies of mixed sodium dodecyl sulfate and N,N-dimethyldodecylamine N-oxide aqueous systems performed at low temperatures, J. Colloid Interf. Sci. 535 (2019) 1–7.

[35] S. Tolle, T. Zuberi, S. Zuberi, W. Warisnoicharoen, M. J. Lawrence, Physicochemical and solubilization properties of n,n-dimethyl-n-(3-dodecylcarbonyloxypropyl)amineoxide: A biodegradable nonionic surfactant, J. Pharm. Sci. 89 (6) (2000) 798–806.

[36] D. J. Barlow, M. J. Lawrence, T. Zuberi, S. Zuberi, R. K. Heenan, Small-angle neutron-scattering studies on the nature of the incorporation of polar oils into aggregates of n,n-dimethyldodecylamine-n-oxide, Langmuir 16 (26) (2000) 10398–10403.

[37] S. K. Singh, M. Rajpai, V. K. Tyagi, Amine oxides: a review, J. Oleo. Sci. 56 (2006) 99 – 119.

[38] W. G., W. J. J., L. F., T. S. S., Development and evaluation of a novel drug delivery: pluronics/sds mixed micelle loaded with myricetin in vitro and in vivo, J. Pharm. Sci. 105 (2016) 1535–43.

[39] S. Khodaparast, W. Sharratt, H. Wang, E. S. Robles, R. Dalgliesh, J. T. Cabral, Spontaneous formation of multilamellar vesicles from aqueous micellar solutions of sodium linear alkylbenzene sulfonate (NaLAS), J. Colloid Interface Sci. 546 (2019) 221 – 230.

[40] O. Arnold, J. C. Bilheux, J. M. Borreguero, A. Buts, S. I. Campbell, L. Chapon, M. Doucet, N. Draper, R. Ferraz Leal, M. A. Gigg, V. E. Lynch, A. Markvardsen, D. J. Mikkelson, R. L. Mikkelson, R. Miller, K. Palmen, P. Parker, G. Passos, T. G. Perring, P. F. Peterson, S. Ren, M. A. Reuter, A. T. Savici, J. W. Taylor, R. J. Taylor, R. Tolchenov, W. Zhou, J. Zikovsky, Mantid—data analysis and visualization package for neutron scattering and μsr experiments, Nucl. Instrum. Meth. A 764 (2014) 156–166.

[41] B. Hammouda, Temperature effect on the nanostructure of SDS micelles in water, J. Res. Natl. Inst. Stan. 118 (2013) 151–167.

[42] H. J. B, P. J., An analytic structure factor for macroion solutions, Molec. Phys. 42 (1) (1981) 109–118.

[43] M. Bergstrom, J. Skov Pedersen, Structure of pure SDS and DTAB micelles in brine determined by small-angle neutron scattering (SANS), Phys. Chem. Chem. Phys. 1 (1999) 4437–4446.

[44] M. Adamo, A. S. Poulos, C. G. Lopez, A. Martel, L. Porcar, J. T. Cabral, Droplet microfluidic SANS, Soft Matter 14 (2018) 1759–1770.

[45] V. Gaikar, K. Padalkar, V. Aswal, Characterization of mixed micelles of structural isomers of sodium butyl benzene sulfonate and sodium dodecyl sulfate by sans, ftir spectroscopy and nmr spectroscopy, Journal of Molecular Liquids 138 (1) (2008) 155 – 167. doi:https://doi.org/10.1016/j.molliq.2007.10.001.
URL http://www.sciencedirect.com/science/article/pii/S0167732207001936

[46] B. H. Tan, K. C. Tam, Y. C. Lam, C. B. Tan, Osmotic compressibility of soft colloidal systems, Langmuir 21 (10) (2005) 4283–4290.

[47] J. Hayter, J. Hansen, A rescaled mean spherical approximation structure factor for dilute charged colloidal dispersion, Molec. Phys. 46 (1982) 651–656.

[48] C. D. Lorenz, C.-M. Hsieh, C. A. Dreiss, M. J. Lawrence, Molecular dynamics simulations of the interfacial and structural properties of dimethyldodecylamine-N-oxide micelles, Langmuir 27 (2) (2011) 546–553.

[49] H. Maeda, Dodecyldimethylamine oxide micelles: stability, aggregation number and titration properties, Colloids and Surfaces A: Physicochemical and Engineering Aspects 109 (1996) 263–271.

[50] K. J. Edler, D. T. Bowron, Temperature and concentration effects on decyltrimethylammonium micelles in water, Molecular Physics 117 (22) (2019) 3389–3397.

[51] J. F. Rathman, D. R. Scheuing, Alkyldimethylamine Oxide Surfactants, Vol. 447, American Chemical Society, 1990, Ch. 7, pp. 123–142.

[52] R. N. A. H. Lewis, R. N. McElhaney, Membrane lipid phase transitions and phase organization studied by fourier transform infrared spectroscopy., Biochim. Biophys. Acta 1828 (10) (2013) 2347–2358.

[53] V. Y. Bezzobotnov, S. Borbely, L. Cser, B. Farago, I. A. Gladkih, Y. M. Ostanevich, S. Vass, Temperature and concentration dependence of properties of sodium dodecyl sulfate micelles determined from small angle neutron scattering experiments, J. Phys. Chem. 92 (20) (1988) 5738–5743.

[54] S. Borbely, L. Cser, S. Vass, Y. M. Ostanevich, Small-angle neutron scattering study of sodium alkyl sulfate mixed micelles, J. Appl. Cryst. 24 (1991) 747–752.

[55] T. Iwasaki, M. Ogawa, K. Esumi, K. Meguro, Interactions between betaine-type zwitterionic and anionic surfactants in mixed micelles, Langmuir 7 (1) (1991) 30–35.

[56] T. R. Desai, S. G. Dixit, Interaction and viscous properties of aqueous solutions of mixed cationic and nonionic surfactants, J. Colloid Interf. Sci. 177 (2) (1996) 471 – 477.

[57] S. Nilsson, K. Thuresson, P. Hansson, B. Lindman, Mixed solutions of surfactant and hydrophobically modified polymer. controlling viscosity with micellar size, J. Phys. Chem. B 102 (37) (1998) 7099–7105.

[58] W. Pabst, E. Gregorová, C. Berthold, Particle shape and suspension rheology of short-fiber systems, Journal of the European Ceramic Society 26 (1) (2006) 149 – 160. doi:https://doi.org/10.1016/j.jeurceramsoc.2004.10.016.
URL http://www.sciencedirect.com/science/article/pii/S0955221904004790

[59] S. Mueller, E. W. Llewellin, H. M. Mader, The rheology of suspensions of solid particles, P. Roy. Soc. A-Math Phy 466 (2116) (2010) 1201–1228.

[60] S. Mueller, E. W. Llewellin, H. M. Mader, The effect of particle shape on suspension viscosity and implications for magmatic flows, Geophysical Research Letters 38 (13) (2011) L13316.

[61] H. Brenner, Rheology of a dilute suspension of axisymmetric brownian particles, Int. J. Mituphase Flow 1 (2) (1974) 195 – 341.

[62] D. Palanisamy, W. K. den Otter, Intrinsic viscosities of non-spherical colloids by brownian dynamics simulations, J. Chem. Phys. 151 (18) (2019) 184902.

[63] T. M. Clausen, P. K. Vinson, J. R. Minter, H. T. Davis, Y. Talmon, W. G. Miller, Viscoelastic micellar solutions: microscopy and rheology, The Journal of Physical Chemistry 96 (1) (1992) 474–484.

[64] J. E. Moore, T. M. McCoy, L. [de Campo], A. V. Sokolova, C. J. Garvey, G. Pearson, B. L. Wilkinson, R. F. Tabor, Wormlike micelle formation of novel alkyl-tri(ethylene glycol)-glucoside carbohydrate surfactants: Structure–function relationships and rheology, Journal of Colloid and Interface Science 529 (2018) 464 – 475. doi:https://doi.org/10.1016/j.jcis.2018.05.060.
URL http://www.sciencedirect.com/science/article/pii/S0021979718305812

[65] M. Kamada, C. Pierlot, V. Molinier, J.-M. Aubry, K. Aramaki, Rheological properties of wormlike micellar gels formed by novel bio-based isosorbide surfactants, Colloids and Surfaces A: Physicochemical and Engineering Aspects 536 (2018) 82 – 87, special issue on Formula VIII. doi:https://doi.org/10.1016/j.colsurfa.2017.07.037.
URL http://www.sciencedirect.com/science/article/pii/S0927775717306866

[66] ISIS Neutron and Muon Source experiments RB1820374.
URL https://doi.org/10.5286/ISIS.E.RB1820374